Intra-Vehicular Path Loss Comparison of UWB Channel for 3–11 GHz and 55–65 GHz

Jiri Blumenstein, Tomas Mikulasek, Ales Prokes
The Faculty of Electrical Engineering and Communication
Brno University of Technology
Brno, Czech Republic
Email: blumenstein@feec.vutbr.cz

Thomas Zemen
AIT Austrian Institute of Technology GmbH,
Vienna, Austria

Christoph Mecklenbräuker
Institute of Telecommunications,
Vienna University of Technology,
Vienna, Austria

***Abstract*—This paper provides a comparison of a real-world intra-vehicular radio channel measurements of the ultra-wide frequency bands, namely the 3–11 GHz and the 55–65 GHz. The measurement campaign was performed utilizing a vector network analyzer (VNA) and a frequency domain method ensuring a high dynamic range of 70 dB and a frequency resolution of 10 MHz. An inverse Fourier transform is exploited for a transition of the measured data into the time domain and to obtain a channel impulse response (CIR). A delay spread and a path loss are derived and compared. Measured data is freely available online: http://www.radio.feec.vutbr.cz/GACR-13-38735S/**

I. Introduction

The inter- and intra-vehicular communication is one of the building blocks of a future smart city infrastructure [1]. Since the amount of wiring inside each vehicle reaches up to several kilometers and weights several tens of kilograms [2], there is a significant effort to replace some of the wire harness with a wireless communication [3]–[6]. This will reduce the weight and consequently also a fuel consumption of vehicles with an internal combustion engine and extend the limited range of electrified vehicles.

A placement of various sensors on the vehicles body and connection of moving parts such as seats, wheels and steering wheel [7] is easier when done wireless. The benefit of wireless connection is also substantiation considering that the wire harnesses of current vehicles is usually platform specific. This feature makes the design and installation of the wire harness a rather demanding process.

As the amount of bandwidth is limited, the potential of high gigahertz bands is growing even despite the unfavorable atmospheric absorption. Therefore, this paper deals with the channel measurement and characterization of the specific in-vehicle environment for the frequency bands of the 3–11 GHz and the 55–65 GHz. Both examined bands offers around 10 GHz of unlicensed bandwidth. However, as we will show in this paper, the radio channel characteristics exhibits notable differences in path loss or delay spread. On one hand, the millimeter wave band suffers from higher atmospheric loss and higher penetration loss compared to the 3–11 GHz band [8], [9]. However, it could benefit from high-gain steerable antennas with small physical dimensions [10]. On the other hand, the 3–11 GHz band provides higher diversity and requires lower transmit power [11].

A. Contribution of the paper

In very similar conditions we compare the 3–11 GHz and the 55-65 GHz frequency bands in terms of:

- The delay spread and root mean square (RMS) delay spread versus antenna separation for the in-vehicle compartment.
- The measured path loss including a comparison with a log-distance path loss model.
- The path loss exponent extraction by means of a maximum likelihood estimate (MLE).
- The measured CIRs for all selected antenna positions.

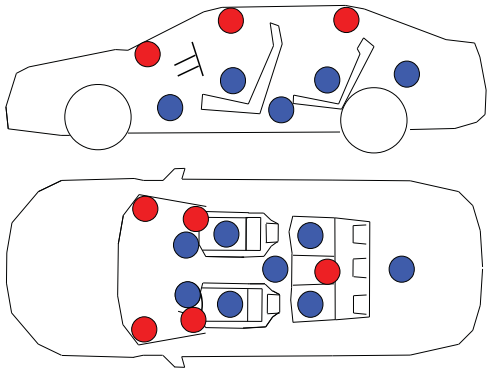

Fig. 1: Antenna placement layout for both 3–11 GHz and 55–65 GHz frequency band. Receiving antennas are depicted in red, transmitting antennas in blue. The VNA is placed outside the vehicle under test. There was no occupancy inside the vehicle during the measurement. The mean antenna separation is 1.28 m while the variance is 0.28 m.

II. Measurement apparatus

The measurements were performed in the mid-sized passenger car Skoda Octavia III. The transmit and receive antennas are marked with red and blue colors in Figure 1 respectively. The receiving (RX) antenna was placed at different spatial points inside the car compartment. The transmitting (TX) antennas were placed on the left and right side of the dash-board and at the rear part of the ceiling according to Figure 1. Please note that the mean antenna separation is 1.28 m while the variance is 0.28 m.

A. 3-11 GHz instrumentation

For each spatial point the s_{41}, s_{42}, and s_{43} scattering parameters corresponding to the channel transfer function (CTF) were measured in the frequency domain utilizing a calibrated four port VNA Agilent Technologies E5071C. The measured radiation patterns of the utilized monoconical antennas are depicted in Figure 2a. The transmitting power was set to 1 dBm.

B. 55-65 GHz instrumentation

The 4-port vector network analyzer R&S ZVA67 was exploited for measuring the transmission coefficient between two antennas in the frequency band 55–65 GHz. The dynamic range of the measurement setup was extended utilizing the broadband power amplifier (QPW-50662330) on the transmitting side. An open waveguide WR15 having the radiation pattern depicted in Figure 2b was utilized as a transmitting and receiving antenna. Here, the transmitting power was set to 13 dBm.

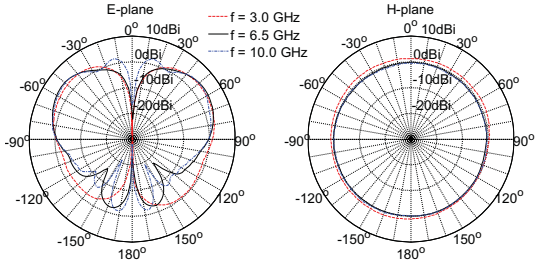

(a) Measured gain pattern of the conical monopole antennas for frequency range 3–11 GHz.

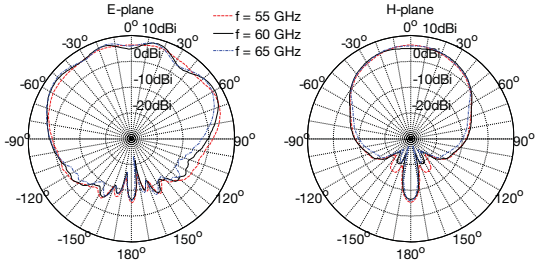

(b) Measured gain pattern of the open ended waveguide in E–plane and H–plane for open ended waveguide antenna at 55–65 GHz.

Fig. 2: Measured radiation patterns of utilized antennas.

III. Channel Parameters

The measurement utilizes swept-frequency channel-sounding method. Thus the CTF is given as:

$$H^{\alpha}(f) = s_{21}^{\alpha}(f), \tag{1}$$

where f represents a measurement index identifiable with certain frequency and where α denotes the position of the receiving antenna within the measured vehicle as depicted in Figure 1. Utilizing an inverse Fourier transform we transform the CTF into a CIR according to:

$$h^{\alpha}(n) = \sum_{f=0}^{N-1} w(f) H^{\alpha}(f) e^{jfn2\pi/N}, \tag{2}$$

where n stands for a discrete time in the delay domain and $w(f)$ represents a Blackman window [12]. Next, we write the definition of the PDP as it will be exploited later in this paper. The power-delay profile (PDP) is given as spatial average of squared CIRs:

$$Q(n) = \mathrm{E}_{\alpha}\{|h^{\alpha}(n)|^2\}. \tag{3}$$

It holds that the time in the delay τ domain is given as $\tau = n/B$, where $1/B$ is the time resolution.

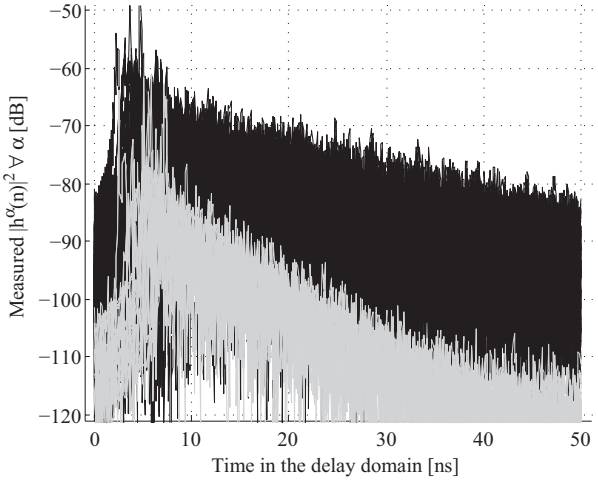

Fig. 4: Overlap of all squared channel impulse responses. The 3–11 GHz are plotted in black, the 55–65 GHz are in gray.

A. Path loss and log-distance path loss model

The path loss or the path attenuation is defined as a difference between transmitted and received power. In free space, this is described by a Friss transmission equation [13]. For the non-free space, the path loss is modeled by the log-distance path loss model. As the path attenuation is specific for each environment and frequency band, the path loss exponent is utilized to determine the particular attenuation. The log-distance path loss model is given as [14]:

$$P(d) = P_{\mathrm{ref}}(d_0) - 10\gamma \log \frac{d}{d_0} + S, \tag{4}$$

where γ is the path loss exponent, d is an antenna separation and S stands for a random process describing a signal fading.

Then, the received power in dBm is calculated from the CIR according to [15]:

$$Pr = 10\log \frac{\sum_{n=0}^{N-1} |h^{\alpha}(n)|^2}{0.001\ R}, \tag{5}$$

where $R = 50\ \Omega$ is the electric resistance of the system. The resulting path loss evaluation is depicted in Figure 5. The respective path loss exponent γ is obtained via MLE fitting. The log-distance path loss model is plotted in a form of solid line together with the measured data. Please note that the x axis is in logarithmic scale. Now, Table I sums the statistical data of the path loss examination.

(a) 3–11 GHz monoconical antenna mounted on front windshield next to the rear-view mirror.

(b) 3–11 GHz monoconical antenna in the middle of the rear seat using a tripod.

(c) The seat behind the front passenger with transmitting open ended waveguide antenna for 55–65 GHz. Please note the heat sink for the power amplifier cooling.

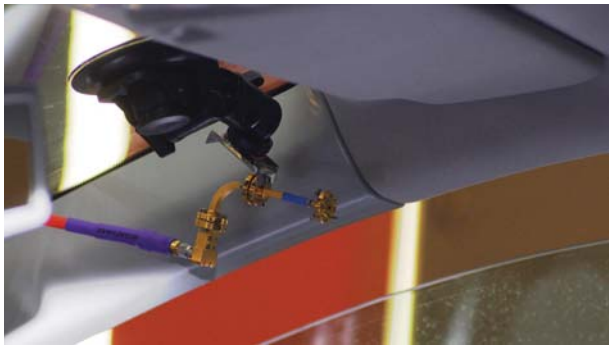

(d) 55–65 GHz open ended waveguide receiving antenna fastened using a suction cap.

Fig. 3: Photographs taken during the measurement campaign.

path loss	mean [dB]	variance [dB]	γ
3-11 GHz	36.37	24.13	20.01
55-65 GHz	52.51	21.40	25.13

TABLE I: Mean and variance of the measured path loss. We derive the path loss exponent γ by means of MLE.

	delay spread		RMS delay spread	
	mean [ns]	variance [ns]	mean [ns]	variance [ns]
3-11 GHz	31.21	10.29	13.18	0.28
55-65 GHz	24.13	4.76	10.05	0.01

TABLE II: Measured delay spread and RMS delay spread values

B. Moments of the PDP

The wireless channel is frequently evaluated via the first and the second central moment of the PDP. The first moment is the mean delay given as [16]:

$$D = \frac{\sum_{n=0}^{N-1} nQ(n)}{\sum_{n=0}^{N-1} Q(n)}, \tag{6}$$

while the second moment of the PDP, the RMS delay spread is defined according to:

$$S_n = \sqrt{\frac{\sum_{n=0}^{N-1} n^2 Q(n)}{\sum_{n=0}^{N-1} Q(n)} - D^2}. \tag{7}$$

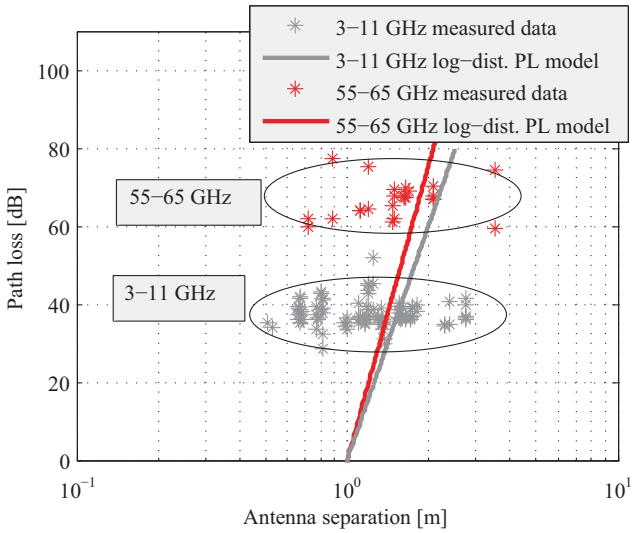

Fig. 5: Path loss evaluation of the 3–11 GHz and the 55–65 GHz band for all antenna positions as depicted in Figure 1 including comparison with the log-distance path loss model (solid lines).

The measured data is plotted in Figure 6 showing around 10 ns higher delay spread in the case of the 3–11 GHz. Detailed statistics are available in Table II.

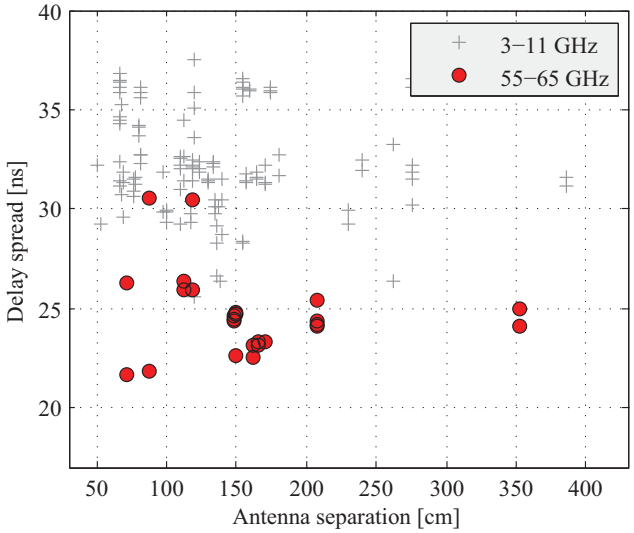

Fig. 6: Delay spread versus antenna separation for the 3–11 GHz band and the 55–65 GHz band.

IV. Conclusion

This paper provides a comparison of the radio channel measurement for the 3–11 GHz and the 55–65 GHz frequency bands inside the passenger vehicle. The channel characteristics are evaluated via the path loss, delay spread, RMS delay spread and CIRs. We also present a parametrization of the path loss utilizing the log-distance path loss model where the path loss exponent is extracted by means of MLE. The mean value of the path loss is 36 dB for the 3–11 GHz band and 52 dB for the 55-65 GHz frequency band. The mean antenna separation is 1.2 m. This measurement takes into account a situation, when the antennas for the 55-65 GHz frequency band are directed to each other while the antennas for the 3–11 GHz band exhibits omnidirectional radiation pattern.

It is worth to note that the variance of the path loss is very similar (approx. 20 dB) for both examined frequency bands. It is also interesting to point out that the log-distance path loss exponent reaches values around 20. It is given by the random placement of the TX-RX antennas inside the vehicle while most of the measured links are non-line of sight (NLOS). Considering the variety of the possible use case scenarios, where the communicating antennas may not be perfectly facing to each other, or in a case of NLOS, the path loss variance is large. Therefore, the validity of the log-distance path loss model for this short-range scenarios is rather poor and the mean path loss with the path loss variance provides more useful information.

The delay spread and the RMS delay spread values for the 3–11 GHz band are 31 ns and 13 ns respectively. For the case of the 55–65 GHz frequency band the delay spread and the RMS delay spread is 24 ns and 10 ns respectively. Also, the variance of the delay spread for the 55–65 GHz band is notably lower, approx. 5 ns compared to 10 ns of the 3–11 GHz band.

To promote a reproducibility of this research, our measured data are freely available online: http://www.radio.feec.vutbr.cz/GACR-13-38735S/.

Acknowledgment

This work was supported by the Czech Science Foundation project No. 13- 38735S Research into wireless channels for intra-vehicle communication and positioning. Research described in this paper was financed by Czech Ministry of Education in frame of National Sustainability Program under grant LO1401. For research, infrastructure of the SIX Center was used. No. CZ.1.05/2.1.00/03.0072, the operational program Research and Development for Innovation. The Christian Doppler Laboratory for Wireless Technologies for Sustainable Mobility is also gratefully acknowledged.

References

[1] C. Sommer and F. Dressler, *Vehicular Networking*.

[2] G. Leen and D. Heffernan, "Expanding automotive electronic systems," *Computer*, vol. 35, no. 1, pp. 88–93, 2002.

[3] E. Ben-Dor, T. Rappaport, Y. Qiao, and S. Lauffenburger, "Millimeter-wave 60 GHz outdoor and vehicle AOA propagation measurements using a broadband channel sounder," in *Global Telecommunications Conference (GLOBECOM 2011), 2011 IEEE*, Dec 2011, pp. 1–6.

[4] M. Schack, M. Jacob, and T. Kurner, "Comparison of in-car UWB and 60 GHz channel measurements," in *Antennas and Propagation (EuCAP), 2010 Proceedings of the Fourth European Conference on*. IEEE, 2010, pp. 1–5.

[5] Y. Katayama, K. Terasaka, K. Higashikaturagi, I. Matunami, and A. Kajiwara, "Ultra-wideband impulse-radio propagation for in-vehicle wireless link," in *Vehicular Technology Conference, 2006. VTC-2006 Fall. 2006 IEEE 64th*, 2006, pp. 1–5.

[6] J. Blumenstein, T. Mikulasek, R. Marsalek, A. Prokes, T. Zemen, and C. Mecklenbrauker, "In-vehicle mm-wave channel model and measurement," in *Vehicular Technology Conference (VTC Fall), 2014 IEEE 80th*. IEEE, 2014, pp. 1–5.

[7] G. Lasser and C. Mecklenbrauker, "Channel model for tyre pressure monitoring systems (TPMS)," in *Antennas and Propagation (EuCAP), 2010 Proceedings of the Fourth European Conference on*. IEEE, 2010.

[8] C. Gustafson, K. Haneda, S. Wyne, and F. Tufvesson, "On mm-wave multipath clustering and channel modeling," *Antennas and Propagation, IEEE Transactions on*, vol. 62, no. 3, pp. 1445–1455, March 2014.

[9] J. Blumenstein, A. Prokes, T. Mikulasek, R. Marsalek, T. Zemen, and C. Mecklenbrauker, "In-vehicle channel measurement, characterization and spatial consistency comparison of 3-11 GHz and 55-65 GHz frequency bands." *IEEE Journal of Selected Topics in Signal Processing - submitted*.

[10] T. Rappaport, J. Murdock, and F. Gutierrez, "State of the art in 60-GHz integrated circuits and systems for wireless communications," *Proceedings of the IEEE*, vol. 99, no. 8, pp. 1390–1436, Aug 2011.

[11] J. Blumenstein, T. Mikulasek, R. Marsalek, A. Chandra, A. Prokes, T. Zemen, and C. Mecklenbrauker, "In-vehicle UWB channel measurement, model and spatial stationarity," in *Vehicular Networking Conference (VNC), 2014 IEEE*. IEEE, 2014, pp. 77–80.

[12] J. Blumenstein, T. Mikulasek, R. Marsalek, A. Prokes, T. Zemen, and C. Mecklenbruker, "Measurements of ultra wide band in-vehicle channel - statistical description and TOA positioning feasibility study," *EURASIP Journal on Wireless Communications and Networking*, 2015.

[13] H. T. Friis, "A note on a simple transmission formula," *proc. IRE*, vol. 34, no. 5, pp. 254–256, 1946.

[14] A. Molisch, D. Cassioli, C.-C. Chong, S. Emami, A. Fort, B. Kannan, J. Karedal, J. Kunisch, H. Schantz, K. Siwiak, and M. Win, "A comprehensive standardized model for ultrawideband propagation channels," *Antennas and Propagation, IEEE Transactions on*, vol. 54, no. 11, pp. 3151–3166, Nov 2006.

[15] T. Gigl, T. Buchgraber, B. Geiger, A. Adalan, J. Preishuber-Pfluegl, and K. Witrisal, "Pathloss and delay-spread analysis of multipath intensive environments using IEEE 802.15.4a UWB Signals," in *COST 2100 Management Committee Meeting*, Sep 2009. [Online]. Available: www.cost2100.org

[16] A. F. Molisch, *Wireless communications*. John Wiley & Sons, 2010, vol. 15.